A Tensor Voting Approach to Dark Spot Detection in RADARSAT-1 Intensity Imagery

Haiyan Guan [1*], Yongtao Yu [2], Jonathan Li[2,3],
[1]School of Geography and Remote Sensing, Nanjing University of Information Science & Technology, Nanjing, Jiangsu 210044, China
[2]School of Information Science and Engineering, Xiamen University, Xiamen, Fujian 361005, China
[3] Department of Geography and Environmental Management, University of Waterloo, Waterloo, ON N2L 3G1, Canada
Email: *guanhy.nj@nuist.edu.cn , allennessy.yu@gmail.com, junli@uwaterloo.ca

***Abstract* —This paper presents a tensor voting approach to automated detection of dark spots in RADARSAT-1 ScanSAR Narrow Beam mode images. First, a thresholding algorithm that well maximizes the ratio of between-class variance to within-class variance is used to detect potential dark spot candidates. Next, a tensor voting framework integrated with sparse and dense ball votings is carried out to suppress noise while maintaining dark spots. Then, a saliency map that reflects the probability of a pixel being located within a dark spot is generated using the saliencies of ball tensors. Finally, a segmentation method is applied to ascertain dark spots based on the saliency map. The proposed approach has been tested on a set of RADARSAT-1 ScanSAR Narrow Beam intensity images. Quantitative evaluations demonstrate that the proposed approach achieves an average commission error, omission error, and quality of 0.003, 0.037, and 0.956, respectively, for detecting dark spots in SAR intensity imagery.**

Index Terms – Dark spot detection, oil spill, tensor voting, perceptual grouping, SAR intensity image

I. INTRODUCTION

The ocean also plays an important role in regulating the Earth's environment and the global climate, as well as providing an essential channel for marine transportation. However, caused by an increasing number of human activities on the ocean, the ocean and its balance are facing terrible changes and destructions. Marine oil pollution, resulting from ship discharges and leakages from oil platforms or oil-tanker accidents, is a major threat to the marine and the coastal ecosystems. Effectively monitoring and managing oil spills is significant to prevent widespread damage from oil pollutions and to reduce the impact on ecosystems. Synthetic aperture radar (SAR) sensors, which can work on all-weather and all-day conditions, have proved to be an efficient and cost-effective way to assist in identifying and monitoring oil spills. The commonly used SAR sensors include RADARSAT-1, RADARSAT-2, ENVISAT, TerraSAR, Cosmos SkyMed, and ERS-2 [1], [2], [3].

Generally, the process of detecting oil spills from SAR imagery is divided into the following three steps [4], [5]: 1) detection of dark spots, which identifies potential oil spill regions in a SAR image; 2) extraction of dark spot features, which generates geometric and statistical representations for each dark spot; and 3) classification of dark spots, which recognizes oil spills from look-alikes according to the extracted features. Dark spot detection is a fundamental and essential procedure in marine oil spill detection and monitoring. Consequently, much effort has been made for dark spot detection in literature. A spatial density thresholding algorithm was developed in [6] to detect dark spots from SAR intensity imagery. In [7], a fully automated algorithm was proposed for dark spot detection by combing the nonadaptive Weibull multiplicative model (WMM) and pulse-coupled neural networks (PCNN). This algorithm first filtered a SAR image based on the WMM, then segmented the image by the PCNN techniques, and finally eliminated the false alarms using a simple filter. A contextual segmentation method was investigated in [8] for detecting dark spots based on histogram analysis of partition features. Similarly, by comparing the histograms of dark spot regions and the sea background, dark spots were detected using a K-distribution model [9].

In this paper, we propose a tensor voting based method for dark spot detection from SAR intensity imagery because tensor voting is capable of inferring geometric structures from noisy and corrupted data. The proposed method has been evaluated on a set of RADARSAT-1 SAR intensity images. The experimental results demonstrate a high performance and accuracy of the proposed method in detecting dark spots of different shapes from SAR intensity images with different types of anomalies.

II. DARK SPOT DETECTION METHOD

The work flow of the proposed dark spot detection method is detailed in Fig. 3. First, a SAR intensity image is binarized to ascertain potential dark spot candidates through intensity thresholding. Second, a saliency map that reflects the probability of a pixel being located within a dark spot is generated after a tensor voting framework. Finally, dark spots are segmented based on the saliency map.

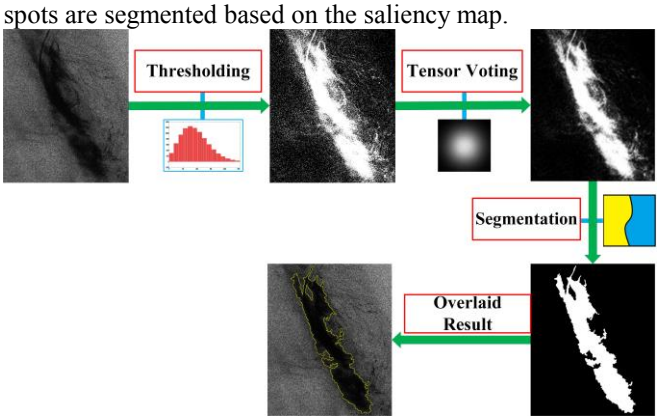

Fig. 1. Flowchart of the proposed dark spot detection method.

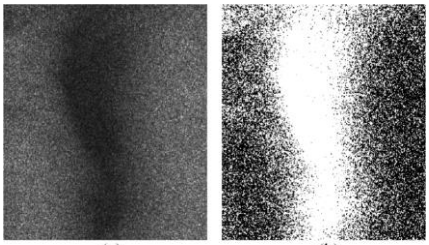

Fig. 2. Illustration of intensity thresholding. (a) Raw SAR intensity image with dark spots, and (b) detected potential dark spot candidates.

A. Intensity Thresholding

As shown in Fig. 2(a), dark spot pixels in a SAR intensity image exhibit relatively lower intensities than those of the background. Generally, the dark pixels, including dark spots and speckle noise, exhibit two types of spatial distributions [5]. Dark pixels that uniformly distribute in a spatial domain are likely to be speckle noise, while the dark pixels that distribute densely within a specific region are deduced to be dark spots. Thus, we use the Otsu's thresholding algorithm to automatically determine an optimal intensity threshold that maximizes the ratio of between-class variance to within-class variance. After the threshold is calculated, the pixels with intensities below the threshold are regarded as potential dark spot candidates, while the others are treated as the background. Fig. 2(b) shows a visual example of the ascertained potential dark spot candidates.

B. Saliency Map Generation

As shown in Fig. 2(b), influenced by speckle noise, a considerable number of pixels are falsely detected as dark spot candidates. Such false alarms should be effectively eliminated in order to identify real dark spots. We propose a tensor voting based algorithm to enhance the contrast between the real dark spots and the false alarms. The tensor voting framework was initially introduced to computer vision for perceptual grouping purposes [10], [11]. In 2D, an arbitrary second-order, symmetric, non-negative definite tensor, which essentially encodes the saliency and orientation of a perceptual structure (e.g. curve, junction, and region), is equivalent to a 2×2 symmetric matrix. The tensor can be decomposed as:

$$\mathbf{T} = \lambda_1 \boldsymbol{e}_1 \boldsymbol{e}_1^T + \lambda_2 \boldsymbol{e}_2 \boldsymbol{e}_2^T = (\lambda_1 - \lambda_2)\boldsymbol{e}_1 \boldsymbol{e}_1^T + \lambda_2 (\boldsymbol{e}_1 \boldsymbol{e}_1^T + \boldsymbol{e}_2 \boldsymbol{e}_2^T) \quad (1)$$

where λ_1 and λ_2 ($\lambda_1 \geq \lambda_2$) are the eigenvalues of the tensor and $\boldsymbol{e}_1$ and $\boldsymbol{e}_2$ are the associated eigenvectors. The first term in (1) corresponds to a stick tensor, which encodes an elementary curve with $\boldsymbol{e}_1$ as its curve normal [10]. The second term corresponds to a ball tensor, which encodes a point located within a region with no preference of orientation or at a junction with multiple orientations.

In the 2D tensor voting framework, a ball tensor represents a perceptual structure of region or junction, and its saliency encodes the probability of a point being located either within a region, which is surrounded by a group of points from the same region, or at a junction where multiple curves intersect and multiple orientations coexist. Therefore, ball tensors can be used to suppress false alarms as well as preserving dark spots simultaneously. The proposed scheme is carried out as follows.

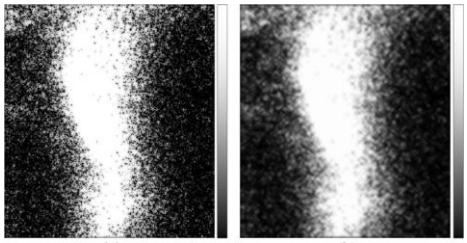

Fig. 3. Illustration of saliency map. (a) Initial saliency map after spare ball voting, and (b) final saliency map after dense ball voting.

Tensor Encoding. The first step is the construction of a voting space. Since no spatial distribution information of the potential dark spot candidates is available, we start by encoding each of the potential dark spot candidates as ball tensors with unit saliencies. In the tensor voting framework, a ball tensor has a perfect circular shape or, analytically speaking, has equal eigenvalues (i.e., $\lambda_1=\lambda_2$) [10]. The tensor directions $\boldsymbol{e}_1$ and $\boldsymbol{e}_2$ are selected arbitrarily because they have no impact on the voting process.

Sparse Ball Voting. Next, we apply a sparse ball voting at each potential dark spot candidate. The ball tensors cast their votes to other tensors within their voting fields, i.e., non-candidates do not join in this voting, which is called sparse ball voting. After sparse ball voting, a general second-order, symmetric, non-negative definite tensor is generated at each

of the potential dark spot candidates. By decomposing the tensors into ball and stick tensor components, we obtain the refined ball tensors with varying saliencies. Based on the saliencies of the refined ball tensors, an initial saliency map reflecting the contrast between the dark spots and the false alarms is constructed, as shown in Fig. 3(a).

Dense Ball Voting. To further refine the saliencies of the initial ball tensors and fill in the gaps between the detected potential dark spot candidates, a dense ball voting, which involves all pixels including potential dark spot candidates and the background into the voting process, is carried out to enhance the contrast between the dark spots and the false alarms. The ball tensors associated with the potential dark spot candidates cast their votes to all the positions within their voting fields. Therefore, both candidates and non-candidates located within the voting field of a ball tensor can receive the votes cast from this ball tensor. After dense ball voting, all the pixels in the SAR intensity image obtain a general tensor that reflects the potential perceptual structures at this pixel. By decomposing the tensors at each pixel into ball and stick tensor components, the final ball tensors that encode the saliencies of a region structure are determined. Consequently, a final saliency map that reflects the probability of a pixel being a dark spot is generated using the saliencies of the final ball tensors, as shown in Fig. 3(b).

Fig. 4. Illustration of segmentation. (a) Initial segmentation result, and (b) final segmentation result.

C. Segmentation

The saliency map (see Fig. 3(b)) reflects the probabilities of the pixels being located within dark spots in a SAR intensity image. The brighter the pixel, the higher the probability. We first apply the Otsu's thresholding algorithm to the saliency map to determine an optimal threshold that well distinguishes dark spot pixels from the background. As shown in Fig. 4(a), after saliency thresholding, some small segments might be incorrectly detected as dark spots. To further remove these false alarms, an area and contrast filter with an area threshold T_A and a contrast threshold T_C is used to refine the segmentation result. The average contrast of the ith detected dark spot is given by [5]:

$$C_i = \frac{u_B - u_i}{\sigma_B}, i = 1, 2, ...n, \quad (2)$$

where n is the number of detected dark spots; u_i denotes the average intensity of the ith dark spot; u_B denotes the average intensity of the background; σ_B denotes the standard deviation of the intensities of the background. Only the segments with an area above T_A and an average contrast above T_C are regarded as real dark spots. Moreover, the small holes inside of the detected dark spots, which are usually generated as a result of errors, are filled in with morphological operations. The final detected dark spots are shown in Fig. 4(b).

III. RESULTS AND DISCUSSION

The SAR intensity images used in this study were captured by the RADARSAT-1 satellite sensors located at the west and east coasts of Canada with an HH polarization. The SAR intensity image dataset, covering vast Pacific and Atlantic coastal areas, contains 93 RADARSAT-1 ScanSAR Narrow Beam images with a swath width of 300 km and a spatial resolution of 50 m. Each of these images contains at least one instance of oil spills or look-alikes indicated by trained human analysts in Canadian Ice Service (CIS) of Environment Canada. The proposed dark spot detection method was applied to these SAR intensity images to detect dark spots. Fig. 5 shows parts of the dark spot detection results from the selected dataset. The sizes of these four images are 560×416, 563×499, 397×506, and 497×844 pixels, respectively. As seen from the thresholding results (see the second row in Fig. 5), many false alarms caused by speckle noise were falsely detected as potential dark spot candidates. Next, we applied the proposed tensor voting framework to the detected potential dark spot candidates to suppress false alarms while preserving dark spots simultaneously. Here, the voting scale σ was set at 5.0, which results in a local vicinity with a radius of approximately 11 pixels. After a combination of sparse and dense ball votings, a saliency map was generated based on the saliencies of the ball tensors (see the third row in Fig. 5). In the saliency maps, the brighter the pixels, the higher the probabilities of the pixels being located within dark spots. Compared to the thresholding results, the saliency maps show high contrast between the real dark spots and the false alarms. The intensities of the pixels belonging to dark spots are dramatically enhanced while the intensities of the pixels belonging to speckle noise are greatly suppressed. Finally, the saliency maps are segmented to ascertain dark spots. In our experiments, we applied the same parameter configurations of T_A=150 and T_C=6.0 to all the test images. The segmented dark spots are shown in the fourth row of Fig. 5.

In order to assess the performance of the proposed method in detecting dark spots, the contours of the detected dark spots were overlaid onto the raw SAR intensity images for visual inspections (see the last row in Fig. 5). Through visual inspection, the proposed method performs well and shows high accuracy in detecting dark spots. To quantitatively evaluate the detection results, a reference

dataset was produced by manual photo-interpretation. However, due to speckle noise and varying contrasts within dark spot regions, manual interpretation can also be very difficult in certain circumstances.

In order to quantitatively evaluate the accuracy of the detection results, we introduce three measures: commission error (E_C), omission error (E_O), and quality (Q). We used the detected dark spot regions, instead of the contours of the dark spots, to evaluate the accuracy of the detection results based on the reference data. The quantitative evaluation results for the SAR intensity images are detailed in Table I. The proposed method achieves a minimal, a maximal, and an average commission errors of 0.000, 0.038, and 0.003, respectively; a minimal, a maximal, and an average omission errors of 0.001, 0.187, and 0.037, respectively; a minimal, a maximal, and an average qualities of 0.852, 0.985, and 0.956, respectively. Thus, the proposed method performs quite well and detects dark spots correctly and accurately.

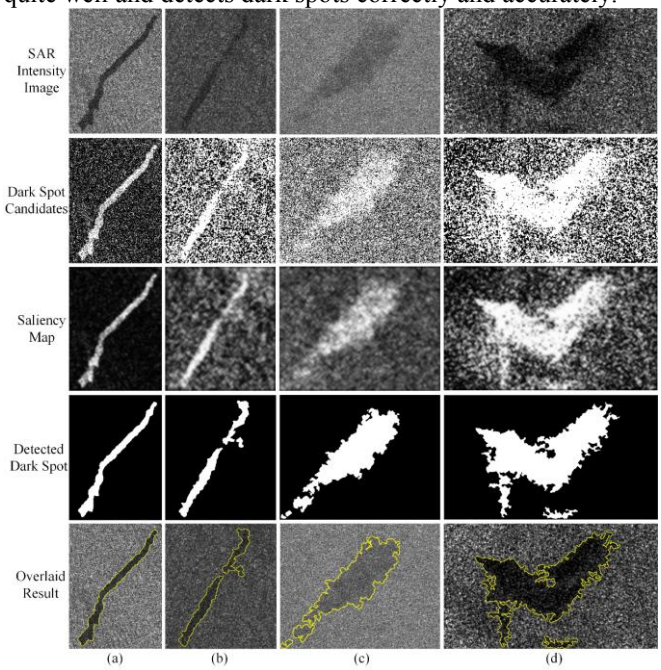

Fig. 5. Parts of dark spot detection results from the SAR intensity image dataset.

TABLE I
QUANTITATIVE EVALUATION RESULTS FOR THE SAR INTENSITY IMAGE DATASET

	Min	Max	Ave.
E_C	0.000	0.038	0.003
E_O	0.001	0.187	0.037
Q	0.852	0.985	0.956

IV. CONCLUSION

In this paper, we have proposed a novel method for detecting dark spots from SAR intensity imagery. Quantitative evaluations have demonstrated that the proposed method achieves an average commission error, omission error, and quality of 0.003, 0.037, and 0.956, respectively, on the RADARSAT-1 dataset. The proposed method was developed using C++ running on an HP Z820 workstation. The average computing time for a SAR intensity image with a size of 100×100 pixels was approximately 2.0 s using only one thread. The time complexity can be further decreased and the performance can be further improved by using parallel computing and multi-thread techniques.

ACKNOWLEDGEMENT

This work was supported by the Startup Foundation for Introducing Talent of Nanjing University of Information Science & Technology (NUIST). The authors would like to thank the Canadian Ice Service of Environment Canada for providing the RADARSAT-1 ScanSAR intensity images.

REFERENCES

[1] L. Xu, J. Li, and A. Brenning, "A comparative study of different classification techniques for marine oil spill identification using RADARSAT-1 imagery," *Remote Sens. Env.*, vol. 141, pp. 14-23, Feb. 2014.

[2] C. Brekke and A.H.S. Solberg, "Oil spill detection by satellite remote sensing," *Remote Sens. Env.*, vol. 95, no. 1, pp. 1-13, Mar. 2005.

[3] K.N. Topouzelis, "Oil spill detection by SAR images: dark formation detection, feature extraction and classification algorithms," *Sensors*, vol. 8, no. 10, pp. 6642-6659, Oct. 2008.

[4] Y. Li and J. Li, "Oil spill detection from SAR intensity imagery using a marked point process," *Remote Sens. Env.*, vol. 114, no. 7, pp. 1590-1601, Jul. 2010.

[5] A.H.S. Solberg, G. Storvik, R. Solberg, and E. Volden, "Automatic detection of oil spills in ERS SAR images," *IEEE Trans. Geosci. Remote Sens.*, vol. 37, no. 4, pp. 1916-1924, Jul. 1999.

[6] Y. Shu, J. Li, H. Yousif, and G. Gomes, "Dark-spot detection from SAR intensity imagery with spatial density thresholding for oil-spill monitoring," *Remote Sens. Env.*, vol. 114, no. 9, pp. 2026-2035, Sep. 2010.

[7] A. Taravat, D. Latini, and F. Del Frate, "Fully automatic dark-spot detection from SAR imagery with the combination of nonadaptive Weibull multiplicative model and pulse-coupled neural networks," *IEEE Trans. Geosci. Remote Sens.*, vol. 52, no. 5, pp. 2427-2435, May 2014.

[8] B. Lounis and A.B. Aissa, "A contextual segmentation of sea SAR images to detect dark spots in Mediterranean Sea," *Proc. Inform. Commun. Tech.*, Damascus, Syria, 2006, pp. 371-376.

[9] H. Li, C. Wang, H. Zhang, F. Wu, and J. Li, "Oil slick spot detection using K-distribution model of the sea background," *Proc. IEEE Int. Geosci. Remote Sens. Symp.*, Cape Town, South Africa, pp. IV-470-IV473.

[10] P. Mordohai and G. Medioni, *Tensor Voting: A Perceptual Organization Approach to Computer Vision and Machine Learning*. USA: Morgan & Claypool, 2006.

[11] R. Moreno, M.A. Garcia, D. Puig, L. Pizarro, B. Burgeth, and J. Wechert, "On improving the efficiency of tensor voting," *IEEE Trans. Pattern Anal. Mach. Intell.*, vol. 33, no. 11, pp. 2215-2228, Nov. 2011.